Optimal Engineered Algae Composition for the Integrated Simultaneous Production of Bioethanol and Biodiesel

Mariano Martín
Dept. de Ingeniería Química, Universidad de Salamanca. Plz., 37008 Salamanca, Spain

Ignacio E. Grossmann
Dept. of Chemical Engineering, Carnegie Mellon University, Pittsburgh, PA15213

DOI 10.1002/aic.14071
Published online April 2, 2013 in Wiley Online Library (wileyonlinelibrary.com)

The optimization of the composition of the algae for the simultaneous production of bioethanol and biodiesel is presented. We consider two alternative technologies for the biodiesel synthesis from algae oil, enzymatic or homogeneous alkali catalyzed that are coupled with bioethanol production from algae starch. In order to determine the optimal operating conditions, we not only couple the technologies, but simultaneously optimize the production of both biofuels and heat integrate them while optimizing the water consumption. Multi-effect distillation is included to reduce the energy and cooling water consumption for ethanol dehydration. In both cases, the optimal algae composition results in 60% oil, 30% starch, and 10% protein. The best alternative for the production of biofuels corresponds to a production price of 0.35 $/gal, using enzymes, with energy and water consumption values (4.00 MJ/gal and 0.59 gal/gal). © 2013 American Institute of Chemical Engineers *AIChE J*, 59: 2872–2883, 2013
Keywords: energy, biofuels, bioethanol, biodiesel, process integration

Introduction

Biofuels are typically classified by the raw materials they use. Thus, corn, vegetable oil, and sugar cane are the raw materials for what has been denoted as first generation fuels. These raw materials have the drawback that they compete with the food supply chain, not only for the land usage for its production, but also for the final product destination, food or biofuel. In order to overcome these limitations, the second generation of biofuels comprises those raw materials that are not used as food product but also does not compete in land with the food supply chain, as they can be grown in marginal areas or wastes from other industries. In this group, we find lignocellulosic raw material such as switchgrass, which can be grown in most of the US territory with good yield, forest residues, corn stover or cooking oil.[1]

The high demand for liquid fuels poses a major challenge on second generation of biofuels due to the limited availability of land and waste. Eventually, there could be a replacement of the use of land for growing energy crops that will affect the food chain leading to food scarcity.[2–5] Cultivating trees and grasses for biofuels may compete with agriculture intended to supply food, feed, and fiber to an expanding world population.[6]

In spite of the promising results reported in the literature for the lignocellulosic based ethanol and FT-diesel[7–12] in terms of energy, water consumption, and low production cost, algae are gaining attention as an alternative source of renewable biomass to increase the production of biofuels and meet the government policies. The use of algae as energy feedstock is not new as it can be traced back to the 1950s.[13] Its main development took place during the oil crisis of 1970s, and the US Department of Energy was funding research on it at the National Renewable Energy Lab (NREL) for more than two decades. The low cost of crude oil closed the program back in 1996 but much has changed since then.[13–15] The great advantage of algae is that they can sequester CO_2 using it as carbon source for the production of biomass, so that these plants can be used alongside fossil fuel power stations,[16,17] or even the CO_2 generated in the production of bioethanol, hydrogen, or FT-diesel from lignocellulosic materials.[10–12,18] Furthermore, the composition of the algae dry matter can be adjusted depending on the algae species and the growth procedure. For instance, microalgae exhibit a great variability in lipid content. Among microalgae species, oil contents can reach up to 80% such as the Botrycoccus and levels of 20–50% are quite common in Chlorella species.[19] The variations are due to different growing conditions and methods of extraction of lipids and fatty acids. Moreover, microalgae like Chlorella, Dunaliella, Chlamydomonas, Scenedesmus, and Spirulina are known to contain a large amount of starch and glycogen (>50% of the dry weight) that can be used as raw materials for ethanol production.[20] Microalgae can also assimilate cellulose which can also be fermented to bioethanol.[13,21]

In a recent paper by Severson et al. (2012),[22] it was shown that the use of bioethanol for the production of biodiesel may be competitive with the use of methanol for a

Correspondence concerning this article should be addressed to Mariano Martín at mariano.m3@usal.es.

production price of ethanol lower than \$0.5/gal. Thus, it is possible to simultaneously define the optimal algae composition together with the integrated production of biodiesel and bioethanol, using part of the bioethanol as transesterifying agent.

In spite of the ideas presented in perspective papers commenting on the integration possibilities within the biorefinery complexes[19,21] and the technological feasibility of the individual processes shown in previous papers,[11,20,22] the actual evaluation of the integrated facilities is still missing in the literature. Furthermore, the simultaneous design and optimization of the integrated process using mathematical programming techniques is expected to provide improved insights on the operation of the biorefinery complex, evaluating tradeoffs related to technology, energy, and water integration. It may also guide future research on algae species[12,19,21] that can allow better process integration by simultaneously optimizing process and the intermediate products. Therefore, in this article we propose the simultaneous optimization and heat integration for the production the two major biofuels, bioethanol and biodiesel, from algae. We evaluate the two most promising processes for the production of biodiesel using ethanol, alkali and enzymatic catalyzed ones from Severson et al.'s paper.[22] We first simultaneously optimize and heat integrate the process from the algae growth to oil extraction, starch depolymerization into glucose and its fermentation to ethanol followed by its dehydration and the transesterification of the oil with ethanol that is self produced. Then, we design the optimal water network to determine the water consumption of the flowsheet, and finally we perform an economic evaluation to fully compare the integrated process with the stand alone process that uses either methanol[23] or ethanol[22] so that we can compare both transesterification agents.

The article is organized as follows. We describe first the superstructure with the different steps involved in the production of oil from algae, bioethanol and biodiesel. Next we discuss the main features of the models. The third part considers the objective function and the solution procedure followed by the results, and the comparison between this integrated process and the use of methanol.

Process Technologies

Figure 1 shows the block diagram of the superstructure for the integrated production of bioethanol and biodiesel from algae. The actual flowsheet including all the different units can be reconstructed using the detailed figures presented along the text. First, algae are grown in ponds. Next, by using an organic solvent the oil is extracted and the starch is separated which is then saccharified and liquefied for the production of ethanol. In parallel, the oil is transesterified using the dehydrated ethanol. We consider the two most promising alternatives for the transesterification of oil using bioethanol,[22] the use of a homogeneous alkali catalyst or the enzymatic catalyzed reaction. The ethanol is recovered, recycled, and mixed with part of the ethanol produced from the starch and the glycerol is separated from the product biodiesel, in this case fatty acid ethyl ester (FAEE).

The units are modeled using an equation-based approach developing reduced order models obtained from experimental data in the literature, design of experiment analysis, mass and energy balances, rules of thumb and design equations due to the complex processes involved in the different stages (i.e., glycerol/FAEE/ethanol equilibrium or the transesterification reaction equilibrium depending on the excess of ethanol, the operating temperature, and the catalyst load), based on the need for having simple and reliable models in order to simultaneously optimize and heat integrate the flowsheet. The superstructure is formulated in terms of the total mass flows, component mass flows, component mass fractions, and temperatures of the streams in the network. The components in the system include {Water, Ethanol, Glycerol, FAEE, FFA, Oil, Hexane, Starch, Glucose, Maltose, Protein, Succinic Acid, Acetic Acid, Lactic Acid, Urea, NH_3, H_2SO_4, KOH, K_2SO_4, H_3PO_4, K_3PO_4, Algae, Biomass, CO_2, O_2}. We describe the main features of the units and the range of the main operating variables. For further details of the models, we refer the reader to previous papers[22–24] where the details of the individual processes can be found. In particular, the production of ethanol from starch shares similarities with first generation of ethanol as starch is also the main component of corn grain, and, therefore, the models for the liquefaction and saccharification of starch, protein separation, and glucose fermentation can be found in Karuppiah et al.[24] The production of biodiesel from algae, the algae growth, the harvesting, and the oil extraction was studied in Martín and Grossmann,[23] while the transesterification of oil using ethanol can be found in Severson et al.[22]

Duran and Grossmann[25] showed that the simultaneous optimization and heat integration can yield significant energy and cost savings. In this process, the recycle of ethanol requires large amount of energy, and, therefore, this motivates the integration of the model presented by Duran and Grossmann[25] in

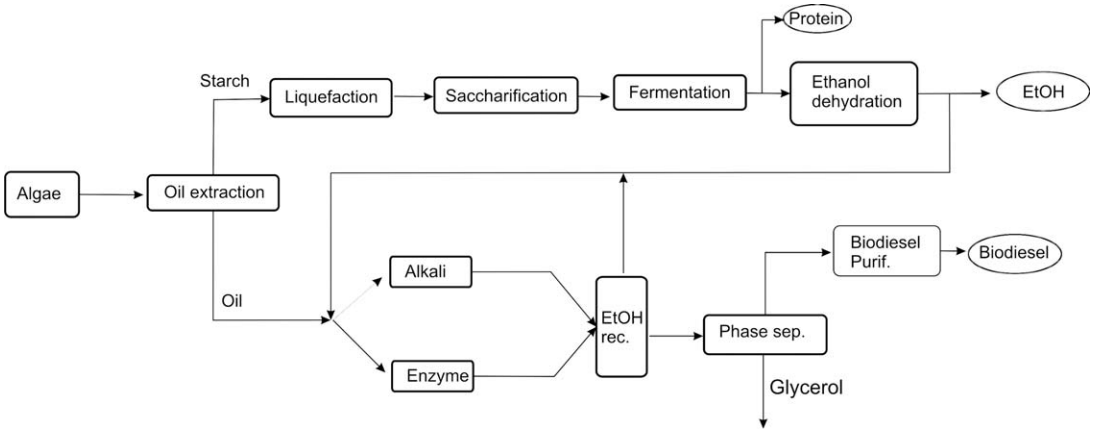

Figure 1. Superstructure for the production of bioethanol and biodiesel from algae.

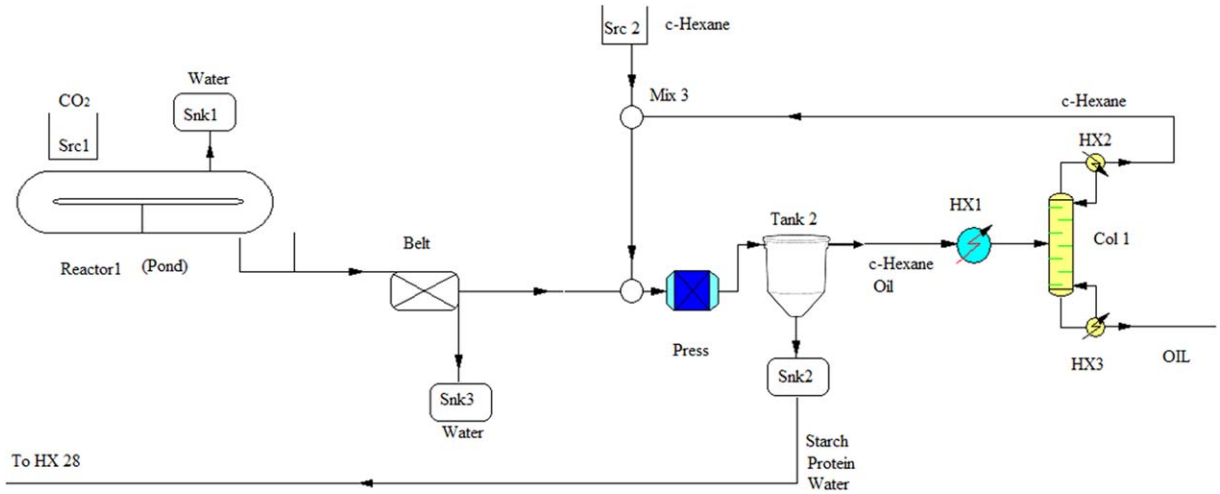

Figure 2. Algae growing and harvesting followed by oil extraction.

[Color figure can be viewed in the online issue, which is available at wileyonlinelibrary.com.]

the problem formulation. Finally, water consumption in biofuels has become another important variable from the environmental and feasibility point of view. The water consumption of this process is also optimized by integrating the energy within the flowsheet followed by the design of the optimal water network based on the results reported by Ahmetović et al. 2010.[26]

Algae production

Figure 2 shows the flowsheet for the production of oil and starch from algae.[23] The production of oil from algae is performed by injecting CO_2 into the water, which can be saline water so that the consumption of freshwater is reduced, together with air and fertilizers. The amount of water needed and the concentration of fertilizers is taken from the report by Pate,[27] while the consumption of CO_2 depends on the growth rate, typically 50 g/m^2 d,[28] and is given by the experimental results by Sazdanoff.[29] We consider a plant size similar to previous papers[22,27] with a dry biomass production of 15 kg/s. Together with the algae, oxygen is produced and water is evaporated.[27] The energy consumed by the pond system is calculated based on the results by Sazdanoff.[29] Next, the algae are harvested from the pond. Recently, Univenture[30] has presented an innovative technology capable of integrating harvesting and drying the algae with low energy consumption. It is based on the use of capillarity, membrane systems, and paint drying to get 5% wet algae with a consumption of 40 W for 500 L/h of flow. The biomass is mixed with cyclo-hexane and pressed so that oil is extracted, and the biomass is separated from the oil. The biomass is sent to liquefaction and saccharification, as we present in the following section, while the oil is used for transesterification and biodiesel production.

One key variable for the process is the ratio starch/oil. This is highly variable depending on the algae species, as well as on the growing conditions.[31] Dragone et al.[32] studied the conditions to regulate the concentration of starch in the algae, and Lv et al.[33] studied the production of lipids. Thus, it is interesting to regulate the amount of starch vs. lipids that can be used in the simultaneous production of ethanol and biodiesel from algae so as to engineer the algae growth for the production of both.[34] We assume that the dry algae consists of starch, which will produce ethanol from fermentation, lipids that will be used for biodiesel production, and protein, that will be used as cattle feed.[35] Thus, the sum of the fractions of the three components in dry basis is equal to 1. The main constraints for the composition of the algae, based on feasible algae in the literature,[33] are the following

$$\begin{aligned} \text{Lipids} &\leq 0.6\,\text{Biomass}_{\text{dry}} \\ \text{Protein} &\geq 0.1\,\text{Biomass}_{\text{dry}} \end{aligned} \tag{1}$$

We assume that the water that accompanies the algae after harvesting can be adjusted so it is appropriate for the fermentation process, considering that this water is part of the algae, and thus not the one used for algae growing.

Transesterification

The oil extracted is transesterified as described by Severson et al.[22] using ethanol as alcohol. In that paper, we identified two promising processes, the use of either alkali or enzymatic catalysts, and thus we will consider both as candidates for the integrated production of bioethanol and biodiesel. For the sake of reducing the length of the article, we describe here only the main features of the process and refer the reader to Severson et al.'s[22] paper for the details

Alkali Based. Figure 3 shows the flowsheet for the synthesis of biodiesel using alkali catalyst. The yield to biodiesel is a function of variables such as operating temperature, ethanol ratio to oil, amount of catalyst. There are a number of trade-offs to obtain a high yield by adjusting the catalyst concentration, ethanol phase, and operating temperature. The catalyst used in reactor 2 is KOH because if neutralized with phosphoric acid, the product precipitates (K_3PO_4). The model for the transesterification reaction is developed based on a design of experiments methods using data from the literature.[36,37] Table 1 shows the range of operation of the variables and the units.

The predicted yield for reactor 2 is given by Eq. 2

$$\begin{aligned} \text{yield} = {} & 22.94293 + 113.88^{*}\text{catalyst} + 2.828881^{*}\text{Ratio\_et} \\ & - 1.02734^{*}\text{Temperature} - 1.44522^{*}\text{catalyst}\,^{*}\text{Ratio\_et} \\ & + 0.250723^{*}\text{catalyst}\,^{*}\text{Temperature} + 0.023375^{*} \\ & \text{Ratio\_et}\,^{*}\text{Temperature} - 41.4402^{*}\text{catalyst}^{\,2} \\ & - 0.07568^{*}\text{Ratio\_et}^{\,2} + 0.006226^{*}\text{Temperature}^{\,2} \end{aligned} \tag{2}$$

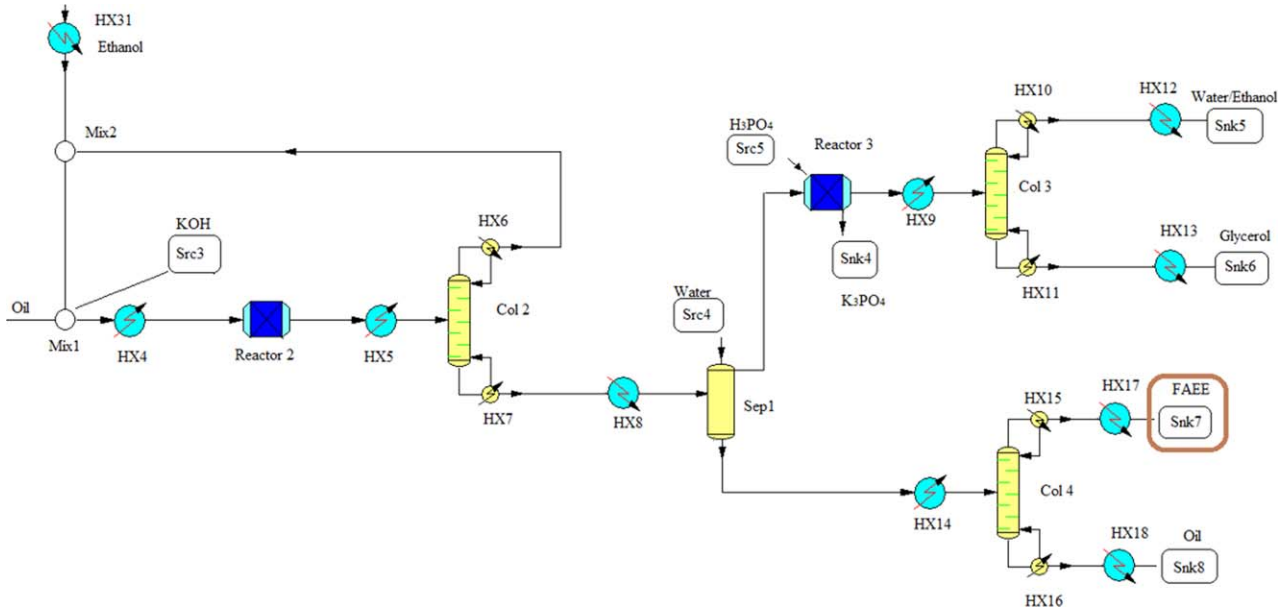

Figure 3. Flowsheet for the production of FAEE using alkali catalyst.

[Color figure can be viewed in the online issue, which is available at wileyonlinelibrary.com.]

The energy involved in the reaction is calculated from the experimental results in the literature.[38] We assume the same value for both technologies. We recover the excess of ethanol in column 2 to be recycled back to the reactor. The columns are modeled using shortcut methods[39] where the operating conditions are defined to avoid thermal decomposition of glycerol. Thus, the temperature at the bottoms must not exceed 150°C, taking into account that we have a two-phase mixture. We assume that at least 94% of the ethanol is recycled. The reflux ratio is set to be greater or equal to 1.2 times the minimum reflux ratio calculated using rules of thumb.[39]

The bottoms are cooled down to 40°C in HX8 before phase separation.[40] The purpose of this stage is to separate the biodiesel from the glycerol, ethanol, and catalyst. Following the typical approach,[41–43] we assume that a water washing column is used to fully separate both phases to eliminate the ions from the catalyst with the polar phase. Phase separation is a difficult stage and there is no agreement whether gravity separation alone can do the work.[41,44] Based on experimental data from Zhou et al.[45] and Cernoch et al.[40], we assume separation between polar and nonpolar phases. A small amount of water, 5% of the biodiesel phase is added to the column.[40]

The oil phase is sent to column 5 to purify the biodiesel from the unreacted oil. To avoid decomposition of the species, the distillate, mainly biodiesel, must exit the column below 250°C while the bottoms, mainly the remaining oil, should remain below 350–375°C. A shortcut model is used for this column assuming a variable reflux ratio from 2 to 3.[42]

The aqueous phase is treated to remove the alkali KOH. We consider the use of phosphoric acid as the neutralization, see Eq. 3, results in K_3PO_4 that can be easily removed using a gravity separator as it precipitates and it can also be sold as a fertilizer

$$H_3PO_4 + 3KOH \rightarrow K_3PO_4 + 3H_2O \quad (3)$$

The products of reactor 3 are calculated based on the stoichiometry of the reaction, and the final temperature is calculated assuming adiabatic operation of the reactor taking into account the heat of neutralization. Once neutralized, the stream is sent to column 3 to purify the glycerol where the bottoms, mainly glycerol, should be kept below 150°C. Furthermore, we are interested in purities above 92% so that glycerol can be sold as a high quality product.[42] The reflux ratio is variable from 2 to 3 and a minimum purity of 0.92 for glycerol is specified.

Enzymatic Based. Similarly, we can use the enzymatic process; see Figure 4 for the detail of the flowsheet. According to Severson et al.,[22] this process is promising in the sense that it consumes less energy and water than the one using KOH, but its current disadvantage is the high cost of the enzymes. The model for the transesterification reactor is given by Eq. 4 developed based on a design of experiment analysis and data from the literature.[46] Table 2 presents the range of operation of the variables and the units.

$$\begin{aligned}\text{yield} = {} & 3.624996 - 1.64904^{*}\text{Temperature} + 17.91299^{*}\text{time} \\ & - 7.60104^{*}\text{Ratio\_et} + 10.59497^{*}\text{catalyst} \\ & - 0.49902^{*}\text{water\_enz} + 0.014332^{*}\text{Temperature}^{2} \\ & - 0.65091^{*}\text{time}^{2} - 0.33241^{*}\text{Ratio\_et}^{2} - 0.31632^{*} \\ & \text{catalyst}^{2} + 0.00692^{*}\text{water\_enz}^{2} - 0.0407^{*} \\ & \text{Temperature}^{*}\text{time} + 0.17485^{*} \\ & \text{Temperature}^{*}\text{Ratio\_et} - 0.0138^{*}\text{Temperature}^{*}\text{catalyst} \\ & - 0.0156^{*}\text{Temperature}^{*}\text{water\_enz} - 0.0601^{*}\text{time} \\ & ^{*}\text{Ratio\_et} - 0.4629^{*}\text{time}^{*}\text{catalyst} + 0.11014^{*}\text{time} \\ & ^{*}\text{water\_enz} + 0.43481^{*}\text{Ratio\_et}^{*}\text{catalyst} + 0.21369^{*} \\ & \text{Ratio\_et}^{*}\text{water\_enz} - 0.09614^{*}\text{catalyst}^{*}\text{water\_enz}\end{aligned} \quad (4)$$

Table 1. Range of Operation of the Variables. Alkali pretreatment

Variable	Lower bound	Upper bound
Temperature (°C)	25	80
Ratio ethanol (mol/mol)	3	20
Catalyst (%w/w)	0.5	1.5

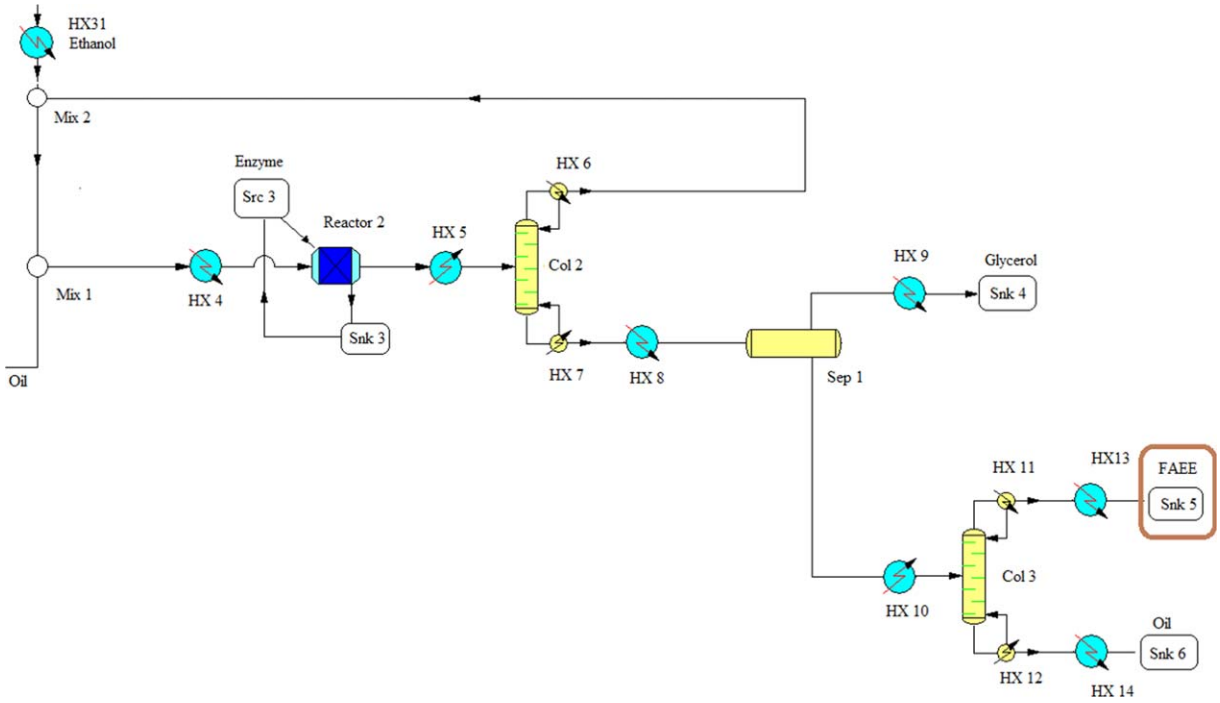

Figure 4. Flowsheet for the production of biodiesel using enzymes.

[Color figure can be viewed in the online issue, which is available at wileyonlinelibrary.com.]

The excess of ethanol is recovered in distillation column 2, and recycled back to the reactor, while the biodiesel is purified by means of gravimetric separation, sep1, and further processes distillation in col3. The main constraints related to product decomposition are the same as from the previous case, with the advantage that the use of supported enzymes, and thus the absence of salts, reduces the purification steps.

Ethanol production

Liquefaction and Saccharification. Liquefaction and saccharification convert the starch to fermentable sugars. This process is similar to the one used for corn ethanol as has been experimentally proved by Maršálková et al.[47] In this model, glucose is considered to be the only sugar. The process consists of two stages, the first one breaks down the starch into maltose and the second one converts maltose into glucose. The liquefaction and saccharification operations are shown in Figure 5. The mass coming from the oil separation stage is fed to the liquefaction tank (*Liq1*), where the high-temperature tolerant enzyme α-amylase is added. The pH range of liquefaction is 6–6.5 and the temperature is kept at 90°C for 30 min.[47–49] The chemical reaction involved in this step is the hydrolysis of starch to maltose, which involves the use of the endoenzyme α-amylase given by Eq. 5

$$2(C_6H_{10}O_5)_n + nH_2O \xrightarrow{\alpha\text{-amylase}} nC_{12}H_{22}O_{11} \qquad (5)$$

Table 2. Range of Operation of the Variables for Enzymatic Process

Variable	Lower bound	Upper bound
Temperature (°C)	20	45
Ratio ethanol (mol/mol)	3	12
Catalyst (%w/w)	5	16
Added water (%w/w)	0	20
Time (h)	6	13

This step is followed by the use of the exoenzyme glucoamylase to achieve the conversion of maltose to glucose in the saccharification process (*Sac1*) given by Eq. 6

$$C_{12}H_{22}O_{11} + H_2O \xrightarrow{\text{glucoamylase}} 2C_6H_{12}O_6 \qquad (6)$$

Saccharification operates most efficiently around 65°C for 30 min.[49] A heat exchanger (*HX29*) cools the mass coming from the liquefaction tank from 90°C to 65°C. The saccharification process is carried out in a pH range of 5.5 for which sulfuric acid is added before the glucoamylase. For the sake of simplicity, we neglect the pH adjustment in the process model. Furthermore, the heats of reaction to obtain glucose from starch are insignificant, and thus neglected in the heat balance.

For the reactions in the liquefaction and saccharification processes, we assume a conversion efficiency of 99% based on the amount of primary reactant.[47] The reactions are modeled on a mass basis and stoichiometric factors are used in the equations. On a mass basis, the reactions are defined by Eqs. 7 and 8.

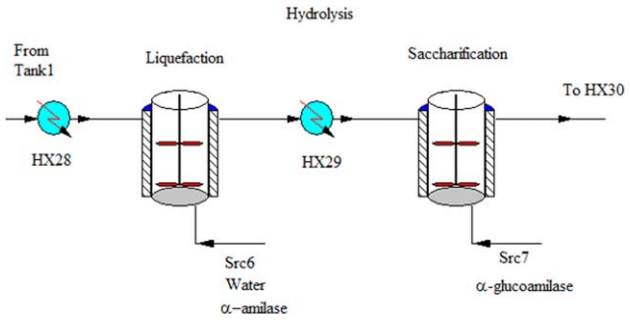

Figure 5. Flowsheet for hydrolysis.

[Color figure can be viewed in the online issue, which is available at wileyonlinelibrary.com.]

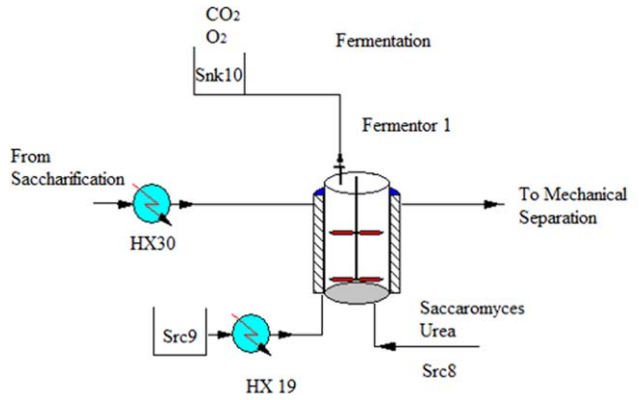

Figure 6. Detail of flowsheet for fermentor.

[Color figure can be viewed in the online issue, which is available at wileyonlinelibrary.com.]

$$1\,\text{kg starch} + 0.0555\,\text{kg water} \xrightarrow{\alpha\text{-amylase}} 1.0555\,\text{kg maltose} \tag{7}$$

$$1\,\text{kg maltose} + 0.0526\,\text{kg water} \xrightarrow{\text{glucoamylase}} 1.0526\,\text{kg glucose} \tag{8}$$

Regarding the enzymes needed in the reactions, the amount of α-amylase to be added is 0.005% w/w of the biomass, while the required glucoamylase is 0.1% w/w of the incoming mash.[49] In the process model, the enzymes are treated as proteins, and hence they are added to the protein mass of the stream. The effect of the enzymes on the energy balance for both the liquefaction and saccharification units is neglected. The mass and heat balances for this section are as follows:

$Wa_{star,malt} = 0.0555$ is the amount of water required for hydrolyzing 1 kg of starch to produce maltose, while $Wa_{malt,gluc} = 0.0526$ is the stoichiometric water requirement for converting 1 kg of maltose into glucose. The terms $conv_{star,malt}$ and $conv_{malt,gluc}$ stand for the conversion of starch to glucose and the conversion of glucose to maltose, respectively, and are both equal to 0.99. $Enz_{Liq} = 0.00005$ is the amount of enzymes (in kg) required per kg of corn mash liquefied, while $Enz_{Sac} = 0.001$ is the amount of enzymes (in kg) required in the saccharification tank per kg of corn slurry saccharified.

Fermentation and Solid Separation. The next step in the production of bioethanol is the fermentation of the slurry. We need to cool down the stream, using heat exchanger *HX30* and then into the fermentor, where yeast and urea are added as well as extra water if needed. The temperature of the slurry entering the fermentor must be 38°C.[48]

The fermentation process is batch, and thus storage tanks are needed to maintain continuous operation of the upstream and downstream processes. Both are considered for the economic evaluation but not described in terms of process modeling. Moreover, the production capacity may result in the need of a train of parallel fermentors. In terms of mass and energy balances, we assume a single fermentor but for costing purposes we will determine the number of fermentors needed for the production capacity. The operations in this part of the flowsheet appear in Figure 6. The loading and unloading of the fermentor are assumed to be instantaneous in the model.

In the fermentor, yeast of the type *Saccharomyces cerevisiae* is used to convert glucose into ethanol. The most often used form is active dry yeast. The amount of yeast used in the fermentor is a function of the amount of corn feed (2.765×10^{-4} kg yeast per kg corn feed processed). The fermentation is assumed to be carried out for a maximum total time of 30 h. During this time, the first 4 h are what is known as a lag phase (*t_lag*), when the incubation of yeast takes place, and hence there is no conversion of glucose to ethanol. In the remaining 26 h (*t_fer_max*), all the glucose is converted into ethanol and a number of by-products. The time dependence of the fermentation reaction is assumed to be linear for the conversion of glucose starting after the initial lag phase of 4 h. The total time (or the cycle time) in the fermentor is then given by

$$t\_cyc = t\_lag + t\_fer \tag{9}$$

There are a number of reactions taking place in the fermentor, see Eq. 10. Table 3 shows the conversions of those reactions

1. Glucose to ethanol : $C_6H_{12}O_6 \xrightarrow{\text{yeast}} 2C_2H_6O + 2CO_2$ $\Delta H = -84.394\,\text{kJ/mol}$
2. Glucose to glycerol : $C_6H_{12}O_6 + 2H_2O \xrightarrow{\text{yeast}} 2C_3H_8O_3 + O_2$
3. Glucose to succinic acid : $C_6H_{12}O_6 + 2CO_2 \xrightarrow{\text{yeast}} 2C_4H_6O_4 + O_2$
4. Glucose to acetic acid : $C_6H_{12}O_6 \xrightarrow{\text{yeast}} 3C_2H_4O_2$
5. Glucose to lactic acid : $C_6H_{12}O_6 \xrightarrow{\text{yeast}} 2C_3H_6O_3$
6. Glucose to cell mass : $C_6H_{12}O_6 + 1.2\,NH_3 \xrightarrow{\text{yeast}} 6\,CH_{1.8}O_{0.5}N_{0.2} + 2.4\,H_2O + 0.3\,O_2$

(10)

In the last reaction of Table 3, ammonia is one of the reactants. This reaction is indicative of the anaerobic growth of the yeast, where the cell mass of the yeast is increased. The ammonia comes from the following reaction that is also assumed to take place inside the fermentor (Eq. 11)

$$\begin{gathered}\text{urea} + \text{water} \xrightarrow{\text{urease}} 2\,\text{ammonia} + \text{carbon dioxide} \\ CO(NH_2)_2 + H_2O \xrightarrow{\text{urease}} 2NH_3 + CO_2\end{gathered} \tag{11}$$

The urea that is required for the reaction is fed through the source *Src7*, from where it goes into the storage tank *Str1* and finally to the fermentor *Fer1*. In order to avoid nitrogen limited growth, we assume that one can feed 10%

Table 3. Chemical Reactions in Fermentor

Reaction	Conversion
$\text{glucose} \xrightarrow{\text{yeast}} 2\,\text{ethanol} + 2\,\text{carbon dioxide}$	0.92
$C_6H_{12}O_6 + 2H_20 \xrightarrow{\text{yeast}} 2C_3H_8O_3 + O_2$	0.034
$C_6H_{12}O_6 + 2CO_2 \xrightarrow{\text{yeast}} 2C_4H_6O_4 + O_2$	0.01
$\text{glucose} \xrightarrow{\text{yeast}} 2\,\text{lactic acid}$	0.002
$\text{glucose} \xrightarrow{\text{yeast}} 3\,\text{acetic acid}$	0.0024
$\text{glucose} + 1.2\,\text{ammonia} \xrightarrow{\text{yeast}} 6\,\text{cell mass} + 2.4\,\text{water} + 0.3\,\text{oxygen}$	0.0316

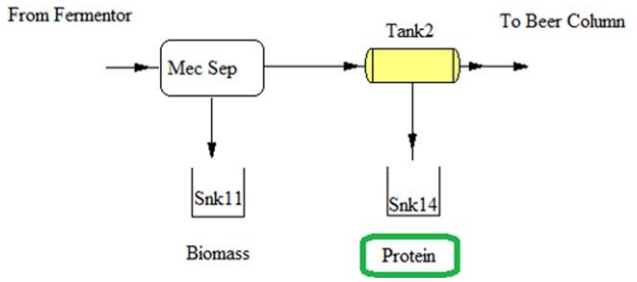

Figure 7. Detail of flowsheet for protein recovery.

[Color figure can be viewed in the online issue, which is available at wileyonlinelibrary.com.]

more urea than what is stoichiometrically required in the fermentor. Besides sugar and nitrogen, other nutrients such as oxygen, and minerals and vitamins are also necessary for efficient fermentation of glucose to ethanol, although in the model the effect of these nutrients is neglected.

Ethanol Purification. Once the liquid stream is separated from the one with solids, we recover the protein by flotation[28] which can be used for cattle feed, see Figure 7. Next, the ethanol must be dehydrated to fuel grade.

Beer Column. Figure 8 shows the scheme of the distillation column. This column is in fact a multi-effect column (Columns 5–7) due to the large energy and water savings reported in previous work.[24,26] The characteristic feature is that the columns operate at different pressures and with different flow rates so that the reboiler of the lower pressure column acts as the condenser of the higher pressure column integrating the heat. Therefore, the main decision variables are the operating pressures at the different column effects to determine a temperature gradient in the intermediate reboilers and condensers to allow heat exchange as well as the fraction of the feed that is processes in each effect. The relative volatility of ethanol with respect to water is taken to be 2.24, and is assumed to be constant over the temperature range of the column. As the two main components of the feed are ethanol and water, we neglect the effect of the other small components such as different acids and glycerol. Therefore, water is chosen to be the heavy key and ethanol the light key for the calculations in both the beer column as well as in the rectification column. The components in small quantities are heavier than water and are assumed to exit through the bottoms. However, due to the small amount we neglect its effect on the vapor-liquid equilibrium. A partial condenser is used in the beer column to obtain a vapor distillate as the molecular sieves handle vapor mixtures of ethanol and water. As a partial condenser is used in the beer column, the composition of the condensed liquid is not the same as the top product, which is removed as saturated vapor. It is assumed that the extracted vapor is in equilibrium with the condensed phase. The composition of the refluxed stream can be calculated by using the vapor-liquid equilibrium relationship for water and ethanol at the temperature of the condenser. The heat loads in the reboiler and the condenser depend on the reflux ratio also, as the recovery of ethanol at the top is fixed at 99.6%, the bottom stream contains almost no ethanol. Thus, only water and ethanol are sent to the final dehydration step. A pressure drop of 10% the operating pressure is assumed for each of the columns. The temperature is calculated as well as the optimal removal of water, while the recovery of ethanol is fixed to be 0.996. With this and the relative volatility, the number of trays of the column is calculated. The temperatures of the inlet and outlet streams are calculated based on bubble and dew point calculations.[39] We consider a partial condenser and the reflux ratio is taken to be (R_{BC1}) of 1.5 according to the results by Karuppiah et al.[24]

Ethanol Dehydratation. For the final dehydration of the ethanol, we use molecular sieves,[11] see Figure 9. There is a lower bound on the fraction of ethanol entering the molecular sieve (0.8). Adsorption takes place at 95°C. Heat exchanger *HX24* heats the inlet stream from the mixer Mix5 up to 95°C. The molecular sieve is a bed of zeolite that operates in semi-continuous mode similar to the cycle described for the corn grit absorbers. The bed is saturated with water after a period of time and is then regenerated. Hence, there are usually two sieves being operated in parallel—one being saturated with water (*MS1*) while the other (*MS1*) is being regenerated (or dehydrated) using air under vacuum. Heat exchanger *HX25* heats air with an assumed relative humidity of 70% at 20°C to 95°C. The air at the outlet of the dehydrating molecular sieve is cooled down to 25°C in heat exchanger *HX26*, and this stream leaves this exchanger saturated with water at 25°C. The data used in the model for the molecular sieves are taken from Jacques et al.[48] and is summarized in Table 4.

Ethanol Production and Recycle. The transesterification operates at 2 to 4 bar. The ethanol coming from the molecular sieves is condensed and mixed with the recycled one in order to provide the ethanol for the production of biodiesel, see Figure 10.

Objective function

The objective function, Eq. 12, is a simplified profit involving income from the production of biodiesel, bioethanol as well as byproducts such as glycerol, protein, and fertilizer and the cost for the consumption of different chemicals, catalysts, and energy (steam); see Table 5 for the data. As we simultaneously optimize and heat integrate the flowsheet, we include the formulation developed by Duran and Grossmann[25] in the problem and, in the objective

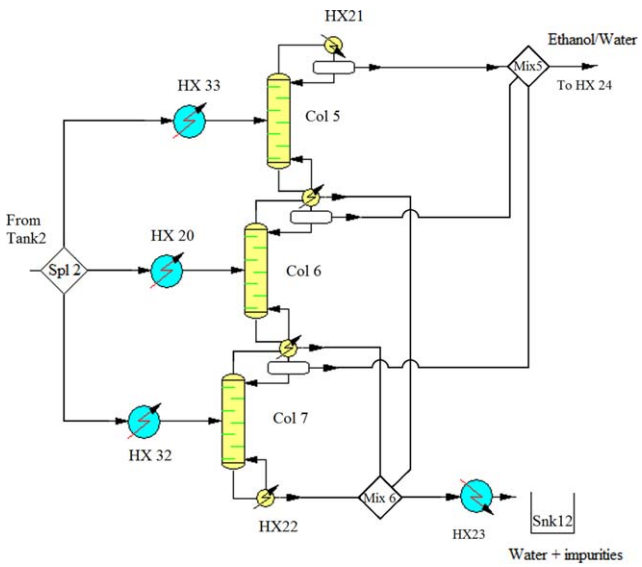

Figure 8. Multi-effect beer column.

[Color figure can be viewed in the online issue, which is available at wileyonlinelibrary.com.]

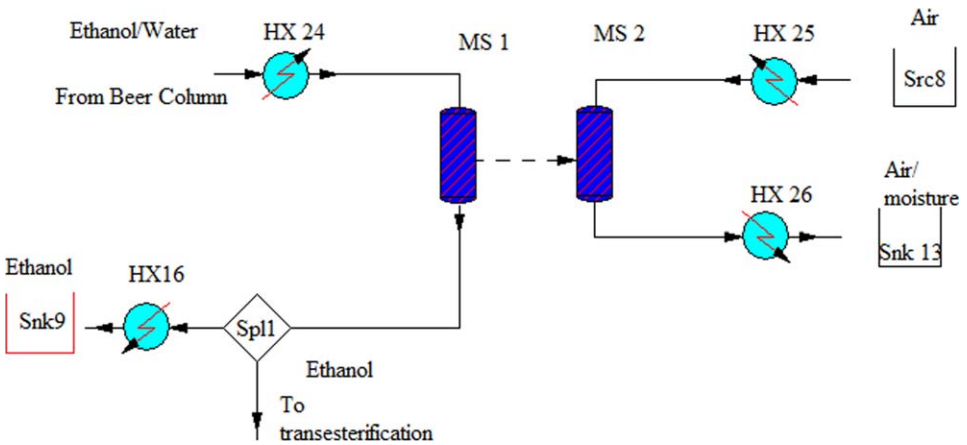

Figure 9. Ethanol dehydration.

[Color figure can be viewed in the online issue, which is available at wileyonlinelibrary.com.]

function, we include QS_max which accounts for the optimal heat integration[39]

$$\begin{aligned} Z = {} & C_{\mathrm{FAME}}{}^{*}\mathrm{fc}\,(\mathrm{FAEE}) + C_{\mathrm{Glycerol}}{}^{*}\mathrm{fc}\,(\mathrm{Glycerol}) \\ & - C_{\mathrm{Steam}}{}^{*}(1/\lambda)^{*}(\mathrm{QS\_max}) - C_{\mathrm{enzy}}{}^{*}\mathrm{Enzymeadded} \\ & {}^{*}\mathrm{f}_{\mathrm{recylce}} + C_{\mathrm{EtOH}}{}^{*}\mathrm{fc}\,(\mathrm{EtOH}) + \mathrm{C}_{\mathrm{Protein}}{}^{*}\mathrm{fc}(\mathrm{Protein}) \\ Z = {} & C_{\mathrm{FAME}}{}^{*}\mathrm{fc}\,(\mathrm{FAEE}) + C_{\mathrm{Glycerol}}{}^{*}\mathrm{fc}\,(\mathrm{Glycerol}) + C_{\mathrm{K_3PO_4}} \\ & {}^{*}\mathrm{fc}\,(\mathrm{K3PO4}) - C_{\mathrm{Steam}}{}^{*}(1/\lambda)^{*}(\mathrm{QS\_max}) \\ & - C_{\mathrm{KOH}} * \mathrm{fc}\,(\mathrm{KOH}) + C_{\mathrm{EtOH}}{}^{*}\mathrm{fc}\,(\mathrm{EtOH}) \\ & - C_{\mathrm{H_3PO_4}}{}^{*}\mathrm{fc}\,(\mathrm{H3PO4}) + \mathrm{C}_{\mathrm{Protein}}{}^{*}\mathrm{fc}(\mathrm{Protein}) \end{aligned} \tag{12}$$

We formulate the superstructure as an MINLP problem involving the mass and energy balances, design equations, yield correlations of all the units described along the text. The problem only has one binary variable to define whether enzymes are used as catalyst for the biodiesel synthesis, or else if KOH is used. In order to provide a comparison between both alternatives, we solve two NLP problems consisting of around 3500 equations and 4100 variables each. The main decision variables are the algae composition in terms of fraction of lipids, carbohydrates and protein to determine the optimal algae composition for the integrated process, the operating temperatures and pressures at the distillation columns and the transesterification reactors, and the composition of the feed to these reactors in order to avoid species decomposition and to optimize the heat integration within the flowsheet. We also include in the flowsheet, a multi-effect column for the dehydration of the ethanol that has proved efficient in reducing the energy and water consumption for bioethanol purification[24,26]. The problem is solved using CONOPT 3.0 for which good initialization points have to be provided.

In order to select one of the two alternatives (transesterification technologies) and to engineer the algae growth, a detailed cost analysis is performed after the optimization involving raw material cost, maintenance, cost of utilities and chemicals, labor, annualized equipment cost and the cost for the management of the facility, following Sinnot's[56] method; see also previous papers by the authors[10] for further details. The prices for facilities are updated from the literature (0.019 \$/kg Steam[57] 0.057 \$/ton cooling water[57], 0.06 \$/kWh[58] 0.021 \$/kg Oxygen[59], 4.876 \$/MMBTU for natural gas.[60] Finally, the cost correlations for the different equipment can be found in the supplementary material of previous papers.[10,23] In a production plant, 0.083 kWh of electricity per gallon of biodiesel[61] is used. Finally, the model by Ahmetović and Grossmann[62] is used in order to design the optimal water network so as to be able to fully compare this integrated process using ethanol with the stand alone process.[23]

Table 4. Data for Molecular Sieves

Parameter	Value
$x_{\mathrm{in,MS}}^{\mathrm{ethanol,min}}$	0.8
$ads\_potential_{\mathrm{MS}}$ (kg water/kg adsorbent)	0.08
$t\_MS_{\mathrm{saturation}}$ (s)	360
$\mathrm{rh}_{\mathrm{in,MS}}$ (%)	70
$\mathrm{rh}_{\mathrm{out,MS}}$ (%)	70

Results

The idea is to engineer the algae composition to drive its growth for the simultaneous production of ethanol and biodiesel, including other byproducts such as glycerol and protein. The prices are given in Table 5. We assume \$1/kg of biofuels, biodiesel, and bioethanol for the objective function. Of particular interest is the price of the byproducts of the process,

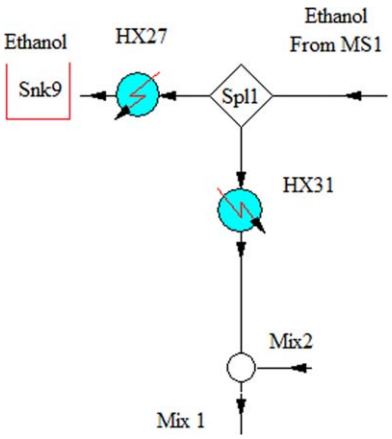

Figure 10. Ethanol split to product of to biodiesel production.

[Color figure can be viewed in the online issue, which is available at wileyonlinelibrary.com.]

Table 5. Chemicals Cost

Chemical	Price ($/kg)	Source
Fertilizer	0.367[a]	Ref. 50
Enzyme	0.7	Ref. 51
KOH	1.6	Ref. 52
H_3PO_4	0.34	Ref. 41
Glycerin	0.3	Ref. 53
c-Hexane	0.41	Ref. 43
Protein	0.2	Ref. 54
K_3PO_4	1.9	Ref. 55

[a]Mean value of a number of fertilizers.

either the protein or the glycerol, whose price is responsible for the final decision on the algae composition. Table 6 presents the distribution of the products and the optimal algae composition. Biodiesel is the main product of the facility with more that 90% of the total biofuel production. Glycerol is a valuable byproduct whose economics determines the profitability of the plant as well as the use of protein. The same algae composition, 60% oil, 30% starch, and 10% protein in the dry biomass, is found for the two alternative trasnesterification technologies. The reasons behind this particular composition are related on the one hand to the high energy consumption for the dehydration of ethanol, so that the system is oriented to the production of as much biodiesel as possible. On the other hand, one can obtain benefit from the biomass remaining after the oil extraction as it contains valuable species that can be further processed to products. Otherwise, a large fraction of the initial biomass is lost. Furthermore, in order for the facility to operate, we need ethanol for the transesterification of the oil and, thus, ethanol is also produced. However, the yield to biodiesel that can be obtained, based on experimental results,[36,37,44] is slightly higher in the case of using alkali catalyst and, therefore, more ethanol is consumed to produce biodiesel.

In Table 7, we present the optimal operating conditions of the multi-effect columns, very similar in both cases which also validate the sequential approach used in previous papers by the authors for the dehydration of the ethanol produced either by sugars or syngas fermentation.[10,11] The main point here is that the operating conditions allow better energy integration with the entire plant as the condenser of the multi-effect column can be used to provide heat to other units, while the reboiler will reduce the need for cooling at the same time as the steam consumption is reduced.

Discussion and Water Consumption

The cost correlations that were used can be found in the supplementary material of previous papers by the authors.[10,23] The first comparison is between the optimal result at the transesterification reactor for the production of biodiesel alone[22] and this integrated flowsheet. Table 8 shows the results. There is no difference in the case of the alkali catalyzed reaction while there is a slight difference in the operating conditions in the case of the enzymatic reactor. The operating temperature is lower in the integrated design and the ethanol ratio in the reactor is half the value in order to improve the energy integration with the rest of the process. The biodiesel production is endothermic requiring energy. If we have to provide that energy at 30°C, more equipment will be able to provide it. There is also difference in terms of the ethanol ratio that determines the energy at the ethanol recovery column and also the temperature.

Freshwater consumption has been gaining attention recently. Despite its low cost, it is becoming scarce in many regions around the world. Optimizing water consumption within a superstructure optimization is difficult due to its low cost and the complexity of simultaneous heat and water integration for large flowsheets.[62] Previous work[26] has shown that energy integration results in freshwater reduction due to the decrease in the cooling needs, taking into account that the main water losses in a process are due to the evaporation losses in the cooling tower. Thus, we use a two stage procedure where, after simultaneous optimization and heat integration, we design the optimal water network to treat and reuse the water that allows determining the freshwater consumption of the facility. We compare this result with the consumption of water of biodiesel plants.[22,23] Therefore, the water consumption is calculated considering the consumption in the cooling tower and the boiler, as well as the amount used in the washing stage of the biodiesel production. We use the model for water network design in the same way as in based on previous work,[30,62] where further information of the models of the utility system design can be found. Figure 11 shows the water network for the enzymatic case. We assume that the water used in the ponds is not fresh, and thus the evaporation losses are not considered for the freshwater balance. We also assume that the water accompanying the cells can be used in hydrolysis and fermentation. However, in order to minimize the water consumption in the

Table 6. Algae Composition and Optimal Product Distribution

	Alkali		Enzymatic	
	Kg/s		Kg/s	
EtOH	0.748		0.868	
Biodiesel	8.555		8.350	
Prot	1.431		1.430	
Glycerol	0.890		0.869	
Algae mass	15	%w/w	15	%w/w
Oil	9	60	9	60
Star	4.5	30	4.5	30
Prot	1.5	10	1.5	10

Table 7. Summary of the Operating Condition of the Distillation Multi-effect Columns

	Column	α	β	P(LP) mmHg	LP/IP	IP/HP
Alkali	Col5–7	0.084	0.238	195	2.13	2.04
Enzymatic	Col5–7	0.084	0.238	182	2.15	2.05

LP: Low pressure; IP: Intermediate pressure; HP: High pressure; α: fraction of total feed to LP column; β: fraction of total feed to IP column.

Table 8. Optimal Operating Conditions

	Alkali catalyzed		Enzymatic	
	Alone (*) (ethanol $1/gal)	Integrated	Alone (*) (ethanol $1/gal)	Integrated
Temperature(°C)	75	75	45	30
Pressure(bar)	4[a]	4[a]	4[a]	4[a]
ratio_et (mol/mol)	5.7	5.7	8.9	4.1
Time (h)	0.5	0.5	6.9	8.0
Cat/lipase(%w/w)	1.5	1.5	14.0	13.0
Water added (%w/w)	–	–	0.0	0.0

[a]fixed condition in the experimental data (*)[22].

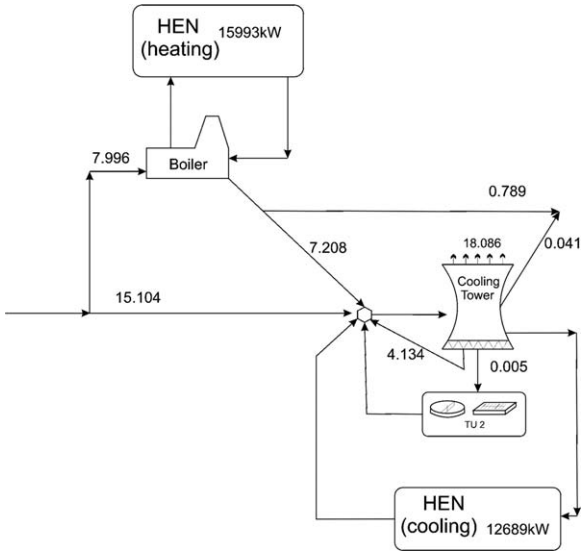

Figure 11. Water network. Enzymatic case. Flows in (t/h).

ponds, there is a closed cycle with the water coming from the distillation column, which is treated using secondary and biological treatment and recycled back to the ponds. Figure 12 shows the partial water network for the enzymatic example.

Table 9 summarizes the production cost, the energy consumption, and the water consumption. As it can be seen, the enzymatic path is almost as expensive as the alkali one, but it is environmentally more friendly due to the lower energy and water consumption. Figure 13 shows the distribution of the cost that justifies the slightly lower cost using the alkali path. It is due to the less expensive KOH catalyst since enzymes are more expensive as they have a short life cycle that requires frequent replacement. Furthermore, the lower cost of the catalysts (KOH vs. Enzyme) and the production of chemicals such as the fertilizers generated in the alkali path and the slightly higher yield to biofuels, provides an advantage for this option in terms of production cost in spite of the lower energy and water consumption. Furthermore, the production of glycerol, protein, and fertilizer as by-products results in negative costs for the chemicals as it is possible to obtain some credit from them.

When we compare the results presented in Table 9 with the ones from the stand alone processes for the production of biodiesel,[22,27] it can be seen that process integration reduces the production cost of biofuel. On the one hand the raw materials are more efficiently used since we use the entire algae composition for biofuel production. On the other

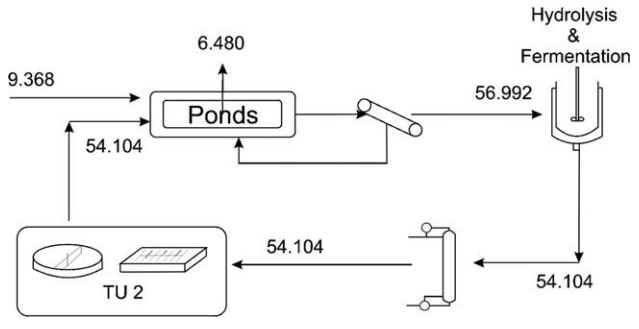

Figure 12. Non freshwater recycle. Enzymatic synthesis. Flows in (t/h).

Table 9. Summary of Results

	Alkali cat	Enzymatic
Production cost ($/gal$_{biofuel}$)	0.32	0.35
Energy (MJ/gal$_{biofuel}$)	6.72	4.00
Water (gal/gal$_{biofuel}$)	0.77	0.59
Investment (MM$)	175	180
Capacity (Mgal/y)	91	90

hand, energy is better integrated. The integrated process presented in this paper still requires energy, and the water consumed is slightly higher than the production of biodiesel alone[22,27] due to the high water demand in the ethanol production section. The enzymatic process is promising, mainly in terms of energy and water consumption compared to the alkali one, but the high cost of the enzyme reduces its profitability. Comparing this process with the production of bioethanol using methanol,[37] the integrated process is competitive in terms of production cost and water consumption ($0.35/gal, 0.59 gal/gal, and 4.00 MJ/gal vs. $0.47/gal, 0.60 gal/gal, and 1.94 MJ/gal for the use of methanol), but it requires more energy due to the pretreatment that the starch needs to access the glucose for fermentation and the dehydration stages for the ethanol.

The investment cost of the processes is calculated following Sinnot's method[56] including equipment cost, installation, piping, instrumentation, based on the estimation for a plant that handles liquids and solids. It turns out to be 175 MM$ and 180 MM$ for the alkali and the enzymatic one for producing 91 and 90 million gallons a year of biofuel, respectively, with 90% corresponding to biodiesel. The investment for an integrated facility that produces bioethanol and biodiesel form algae is higher than the production of biodiesel alone[22] but in the range of the production of biochemical second generation bioethanol production for a lower total biofuels production capacity, usually limited by the availability of raw material to 60 MMgal year, as well as below the ones for bioethanol (335$MM) or FT-diesel (216MM$) production from gasification of switchgrass also for 60 MMgal/yr.[10,12] Figure 14 presents the breakdown of the investment cost for the enzyme case into different stages of the process, from algae growth, harvesting and oil extraction, oil transesterification, ethanol production, ethanol dehydration, and finally the heat exchanger network. We would like to point out that energy integration prevents a complete separation of the stages as the energy is expected to be reused within the process, and thus the heat exchangers are shared between them. Apart from this small drawback, it is important to highlight the large contribution of the ponds to the investment cost while biodiesel production has the lowest share, which together with the high energy consumption for ethanol dehydration, supports the fact that algae composition is driven by the lipids' production.

Conclusions

We have analyzed two paths, alkali or enzymatic catalyzed, for the simultaneous production of bioethanol and biodiesel from algae to engineer the algae composition toward the optimal distribution of products. We propose the integrated production including algae growth, oil transesterification, ethanol recovery and biodiesel purification, and starch treatment, fermentation, and ethanol dehydration by means

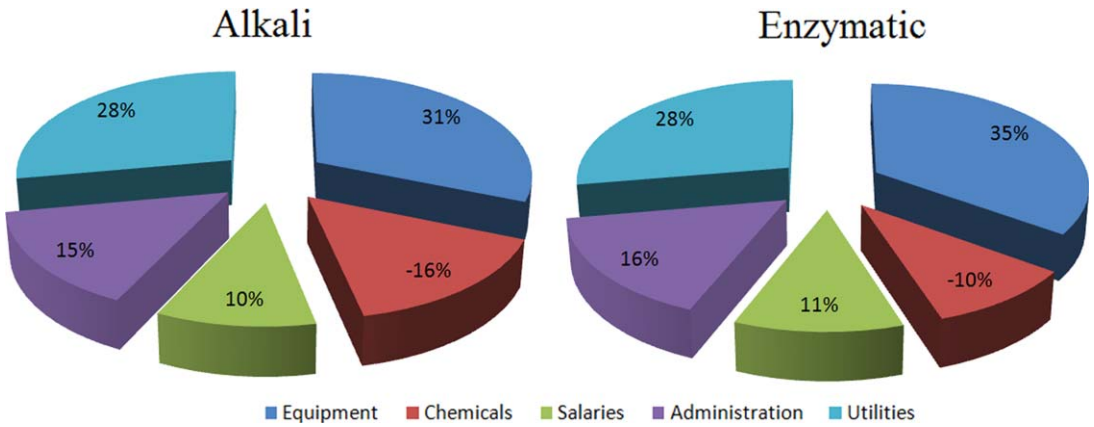

Figure 13. Production cost distribution.

[Color figure can be viewed in the online issue, which is available at wileyonlinelibrary.com.]

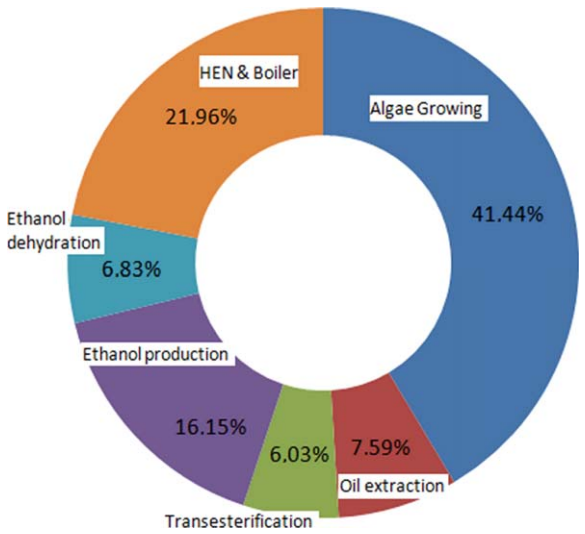

Figure 14. Break down of the investment by stages.

[Color figure can be viewed in the online issue, which is available at wileyonlinelibrary.com.]

of multi-effect columns and molecular sieves with simultaneous optimization and heat integration.

The optimal algae composition in dry matter corresponds to 60% oil, 30% starch, and 10% protein no matter what production path is selected. However, we acknowledge that it may depend on the product and byproduct prices (glycerol and protein). Among the two alternatives for biodiesel production, both are similar in terms of production cost, but the enzymatic catalyzed reactor requires less energy and water (4.00 MJ/gal and 0.59 gal/gal, respectively) and is, therefore, the process of choice.

Even though the integrated process requires higher energy and water consumption, the simultaneous production of ethanol and biodiesel is more advantageous than the production of biodiesel using ethanol alone as it reduces the biofuel production cost around 20%, mostly because of the reduction in the raw material cost.

Acknowledgments

The authors gratefully acknowledge support from the National Science Foundation Grant CBET0966524 and from the Center for Advanced Process Decision-making at Carnegie Mellon University. Dr. M. Martin gratefully acknowledges the financial support from the University of Salamanca Research for software licenses.

Literature Cited

1. Nigam PS, Singh A. Production of liquid biofuels from renewable resources. *Prog Energy Combust Sci*. 2011;37(1):52–68.
2. Donner SD, Kucharik CJ. Corn-based ethanol production compromises goal of reducing nitrogen export by the Mississippi River. *Proc Natl Acad Sci. USA* 2008;105:4513–4518.
3. Fargione J, Hill J, Tilman D, Polasky S, Hawthorne P. Land clearing and the biofuel carbon debt. *Science* 2008;319:1235–1238.
4. Landis DA, Gardiner MM, van der Werf W, Swinton SM. Increasing corn for biofuel production reduces biocontrol services in agricultural landscapes. *Proc Natl Acad Sci. USA* 2008;105:20552–20557.
5. Searchinger T, Heimlich R, Houghton RA, Dong F, Elobeid A, Fabiosa J, Tokgoz S, Hayes D, Yu TH. Use of US croplands for biofuels increases greenhouse gases through emissions from land-use change. *Science*. 2008;319:1238– 1240.
6. Sheehan J. Engineering direct conversion of CO_2 to biofuel. *Nat Biotechnol*. 2009;27:1128–1129.
7. Aden A, Foust T. Technoeconomic analysis of the dilute sulfuric acid and enzymatic hydrolysis process for the conversion of corn stover to ethanol. *Cellulose* 2009;16:535–545.
8. Phillips S, Aden A, Jechura J, Dayton D, Eggeman T. Thermochemical ethanol via indirect gasification and mixed alcohol synthesis of lignocellulosic biomass. *Technical Report*, NREL/TP-510–41168, April 2007.
9. Dutta A, Phillips SD. Thermochemical ethanol via direct gasification and mixed alcohol synthesis of lignocellulosic biomass. *Technical Report*, NREL/ TP-510–45913, 2009.
10. Martín M, Grossmann IE. Energy optimization of Bioethanol production via gasification of switchgrass. *AIChE J*. 2011;57(12):3408–3428.
11. Martín M, Grossmann IE. Energy optimization of ethanol production via hydrolysis. *AIChE J*. 2012;58(5):1538–1549.
12. Martín M, Grossmann IE. Process optimization of FT diesel production from lignocellulosic switchgrass. *Ind Eng Chem Res*. 2011; 50(23):13485–13499.
13. Chen P, Min M, Chen Y, Wang L, Li Y, Chen Q, Wang C, Wan Y, Wang X, Cheng Y, Deng S, Hennessy K, Lin X, Liu Y, Wang Y, Martinez B, Ruan R. Review of the biological and engineering aspects of algae to fuels approach. *Int J Agric Biol Eng*. 2009;2:1–30.
14. Waltz E. Biotech's green gold? *Nat. Biotechnol*. 2009;27:15–18.
15. Knoshaug EP, Darzins A. *Algal Biofuels: The Process. CEP*. 2011:37–47.
16. Sawayama S, Inoue S, Dote Y, Yokoyama SY. CO_2 fixation and oil production through microalgae. *Energy Convers Manage*. 1995;36:729–731.
17. Brown LM, Zeiler. KG. Aquatic biomass and carbon dioxide trapping. *Energy Convers Manage*. 1993;34:1005–1013.

18. Martín M, Grossmann IE Energy optimization of Hydrogen production from biomass. *Comp Chem Eng*. 2011;35(9):1798–1806.
19. Powell EE, Hill GA. Economic assessment of an integrated bioethanol–biodiesel–microbial fuel cell facility utilizing yeast and photosynthetic algae. *Chem Eng Res Des.* 2009;87:1340–1348.
20. Ueda R, Hirayama S, Sugata K, Nakayama H. Process for the production of ethanol from microalgae, 1996, *US Patent* 5,578,472.
21. Cardona-Alzate CA, Sánchez-Toro OJ. Energy consumption analysis of integrated flowsheets for production of fuel ethanol from lignocellulosic biomass. *Energy*. 2006;31:2447–2459.
22. Severson K, Martin M, Grossmann IE. Optimal production of biodiesel using bioethanol. *AICHE J*. 2012;59:834–844.
23. Martín M, Grossmann IE. Simultaneous optimization and heat integration for biodiesel production from cooking oil and algae. *Ind Eng Chem Res*. 2012;51:7998–8014.
24. Karuppiah R, Peschel A, Grossmann IE, Martín M, Martinson W, Zullo L, Energy optimization of an ethanol plant. *AICHE J*. 2008;54:1499–1525.
25. Duran MA, Grossmann IE. Simultaneous optimization and heat integration of chemical processes. *AIChE J*. 1996;32:123–138.
26. Ahmetović E, Martin M, Grossmann IE. Optimization of energy and water consumption in corn-based ethanol plants. *Ind Eng Chem Res*. 2010;49(17):7972–7982.
27. Pate R. Biofuels and the energy–water nexus. In: AAAS/SWARM, April 11, 2008 Albuquerque, NM.
28. Schenk PM, Thomas-Hall SR, Stephens E, Marx UC, Mussgnug JH, Posten C. Kruse O, Hankamer B. Second generation biofuels: high-efficiency microalgae for biodiesel production. *Bioenerg. Res.* 2008;1:20–43.
29. Sazdanoff N. Modeling and simulation of the algae to biodiesel fuel cycle. Undergraduate Thesis, The Ohio State University, 2006.
30. Univenture. *Harvesting, Dewatering, and Drying Technology*, Univenture, 2009. http://diogenesinstitute.org/images/e/e3/Avs_harvester_tech_expl.pdf. Last accesed March 2013.
31. John RP, Anisha GS, Nampothiri KM, Pandey A. Micro and macroalgal biomass: a renewable source for bioethanol. *Bioresour Technol*. 2011;102:186–193.
32. Dragone G, Fernandes BD, Abreu AP, Vicente AA, Teixeira JA. Nutrient limitation as a strategy for increasing starch accumulation in microalgae. *Appl Energ*. 2011;88(10):3331–3335.
33. Lv J-M, Cheng L-H, Xu X-H, Zhang L, Chen HL. Enhanced lipid production of *Chlorella vulgaris* by adjustment of cultivation conditions. *Bioresour Technol*. 2010;101:6797–6804.
34. Beer LL, Boyd ES, Peters JW, Posewitz MC. Engineering algae for biohydrogen and biofuel production. *Curr Opin Biotech*. 2009;20:264–271.
35. McKendry P. Energy production from biomass (part 2): conversion technologies. *Bioresour Technol*. 2002;83:47–54.
36. Silva NL, Batistella CB, Filho RM, Maciel MRW. Biodiesel production from castor oil: optimization of alkaline ethanolysis. *Energy Fuels*. 2009;23:5636–5642.
37. Joshi HC, Toler J, Walker T. Optimization of cottonseed oil ethanolysis to produce biodiesel high in gossypol content. *J Am Oil Chem Soc*. 2008;85:357–363.
38. Dalai AK. Applications of Vegetable Oil Derived Esters as a Diesel Additive. *Energeia* 2004;15(5):1–6. Available at: http://www.caer.uky.edu/energeia/PDF/vol15_6.pdf.
39. Biegler LT, Grossmann IE, Westerberg AW. *Systematic Methods of Chemical Process Design*. New Jersey: Prentice Hall. 1997.
40. Cernoch M, Skopal F, Hájek M. Separation of reaction mixture after ethanolysis of rapeseed oil. *Eur J Lipid Sci Technol*. 2009;111:663–668.
41. West AH, Posarac D, Ellis N. Assessment of four biodiesel production processes using HYSYS.Plant. *Bioresour Technol*. 2008; 99: 6587–6601.
42. Zhang Y, Dube MA, McLean DD, Kates M. Biodiesel production from waste cooking oil: 1. process design and technological assessment. *Bioresour Technol*. 2003;89:1–16.
43. Zhang Y, Dube MA, McLean DD, Kates M. Biodiesel production from waste cooking oil: 2. economic assessment and sensitivity analysis. *Bioresour Technol*. 2003;90:229–240.
44. Krawczyk T. Biodiesel alternative fuel makes inroads but hurdles remain. *Inform* 1996;7(8):801–815.
45. Zhou W, Boocock DGB. Phase behavior of the base-catalyzed transesterification of soybean oil. *J Am Oil Chem Soc*. 2008;83(12):1041–1045.
46. Rodrigues RC, Volpato G, Ayub MAZ, Wada K. Lipase-catalyzed ethanolysis of soybean oil in a solvent-free system using central composite design and response surface methodology. *J Chem Technol Biotechnol*. 2008;83:849–854.
47. Maršálková B, Širmerová M, Kuřec M, Brányik T, Bányiková I, Melzoch K, Zachleder, V. Microalgae *Chlorella sp*. as an alternative source of fermentable sugars. *Chem Eng Trans*. 2010;21:1279–1285.
48. Jacques K, Lyons TP, Kelsall DR. *The Alcohol Textbook*, 3rd ed., Nottingham, UK: Nottingham University Press, 1999.
49. Choi SP, Nguyen MT, Sim SJ. Enzymatic pretreatment of Chlamydomonas reinhardtii biomass for ethanol production. *Bioresour Technol*. 2010;101:5330–5336.
50. American Crystal Sugar Company: NPK/Fertilizer Calculator. Last accesed March 2013. Available at: http://www.crystalsugar.com/agronomy/agtools/npk/Default.aspx.
51. Sotoft LF, Rong BG, Christensen KV, Norddahl, B. Process simulation and economical evaluation of enzymatic biodiesel production plant. *Bioresour Technol*. 2010;101(14):5266–5274.
52. Available at: http://www.alibaba.com/showroom/koh-food-grade.html. Last accessed March 2013.
53. Taylor, J., 2012 Sample Report Glycerine (US Gulf). http://www.icispricing.com/il_shared/Samples/SubPage170.asp. Last accessed March 2013.
54. USDA 2011 Available at: www.extension.iastate.edu/agdm. Last accessed March 2012.
55. Available at: http://www.sunivo.com/ennew/Products/Products_list.asp?sProdKw=potassium phosphate. Accessed December 2011.
56. Sinnot RK. *Coulson and Richardson, Chemical Engineering*. *3rd ed*. Singapore: Butterworth Heinemann, 1999.
57. Franceschin G, Zamboni A, Bezzo F, Bertucco A. Ethanol from corn: a technical and economical assessment based on different scenarios *Chem Eng Res Des*. 2008;86(5):488–498.
58. Balat M, Balat H, Öz, C. Progress in bioethanol processing. *Prog Energy Combust Sci*. 2008;34(5):551–573.
59. Piccolo C, Bezzo F. A techno-economic comparison between two technologies for bioethanol production from lignocelluloses. *Biomass Bioenergy* 2009;33:478 – 491.
60. Williams JL. 2013. http://www.wtrg.com/daily/gasprice.html. Available at: http://www.wtrg.com/daily/gasprice.html. Last accessed March 2013.
61. Radich A. *Biodiesel Performance, Costs, and Use*. Available at: http://tonto.eia.doe.gov/ftproot/environment/biodiesel.pdf (accessed July 2010).
62. Ahmetović E, Grossmann IE. Global superstructure optimization for the design of integrated process water networks. *AIChE J*. 2011;57(2):434–457.

Manuscript received Nov. 18, 2012, and revision received Feb. 6, 2013.